Received: 5 February 2023 | Revised: 8 April 2023 | Accepted: 27 May 2023

DOI: 10.1111/cas.15881

Cancer Science WILEY

ORIGINAL ARTICLE

LncRNA-HOTAIRM1 promotes aerobic glycolysis and proliferation in osteosarcoma via the miR-664b-3p/Rheb/mTOR pathway

Xuecheng Yu[1] | Weihao Duan[1] | Furen Wu[1,2] | Daibin Yang[1,2] | Xin Wang[1] | Jingbin Wu[1] | Dong Zhou[3,4,5] | Yifei Shen[1]

[1]Department of Orthopedics, The Affiliated Changzhou Second People's Hospital of Nanjing Medical University, Changzhou Medical Center, Nanjing Medical University, Changzhou, China

[2]Dalian Medical University, Dalian, China

[3]Changzhou No.6 People's Hospital, Nanjing Medical University, Changzhou, China

[4]Changzhou Medical Center, Nanjing Medical University, Changzhou, China

[5]Department of Orthopedics, Wuqia People's Hospital, Xinjiang, China

Correspondence
Dong Zhou, Changzhou No.6 People's Hospital, Changzhou Medical Center, Nanjing Medical University, Changzhou, 213003, China.
Email: zhoudong1012@163.com

Yifei Shen, Department of Orthopedics, The Affiliated Changzhou Second People's Hospital of Nanjing Medical University, Changzhou Medical Center, Nanjing Medical University, Changzhou, 213003, China.
Email: nydshenyifei@163.com

Funding information
Changzhou Medical Center project, Grant/Award Number: CMCB202216; National Natural Science Foundation of China, Grant/Award Number: 82160555; Natural Science Foundation of Xinjiang Province, Grant/Award Number: 2022D01A317

Abstract

Osteosarcoma (OS), which is a common and aggressive primary bone malignancy, occurs mainly in children and adolescent. Long noncoding RNAs (lncRNAs) are reported to play a pivotal role in various cancers. Here, we found that the lncRNA HOTAIRM1 is upregulated in OS cells and tissues. A set of functional experiments suggested that HOTAIRM1 knockdown attenuated the proliferation and stimulated the apoptosis of OS cells. A subsequent mechanistic study revealed that HOTAIRM1 functions as a competing endogenous RNA to elevate ras homologue enriched in brain (Rheb) expression by sponging miR-664b-3p. Immediately afterward, upregulated Rheb facilitates proliferation and suppresses apoptosis by promoting the mTOR pathway-mediated Warburg effect in OS. In summary, our findings demonstrated that HOTAIRM1 promotes the proliferation and suppresses the apoptosis of OS cells by enhancing the Warburg effect via the miR-664b-3p/Rheb/mTOR axis. Understanding the underlying mechanisms and targeting the HOTAIRM1/miR-664b-3p/Rheb/mTOR axis are essential for OS clinical treatment.

KEYWORDS
HOTAIRM1, miR-664b-3p, mTOR, osteosarcoma, Rheb

Abbreviations: CCK-8, Cell-Counting Kit-8; ECAR, extracellular acidification rate; FBS, fetal bovine serum; FISH, fluorescence in situ hybridization; FTI, Farnesyltransferase inhibitor; GEO, Gene Expression Omnibus; HOTAIRM1, HOXA transcript antisense RNA myeloid-specific 1; IHC, immunohistochemistry; lncRNA, long noncoding RNA; miRNA, microRNA; OCR, oxygen consumption rates; OS, osteosarcoma; qRT-PCR, quantitative real-time polymerase chain reaction; Rheb, Ras homologue enriched in brain; TUNEL, terminal deoxynucleotidyl transferase dUTP nick-end labeling.

Xuecheng Yu, Weihao Duan, Furen Wu, and Daibin Yang have contributed equally to this work and share the first authorship.

1 | INTRODUCTION

Osteosarcoma (OS), the most common and aggressive type of primary malignant bone tumor, arises most often in children and adolescents.[1,2] It is derived from interstitial tissue and is characterized by heterogeneity, rapid progression, and a high risk of metastasis, primarily to the lungs.[3] Nevertheless, the underlying molecular mechanisms of OS pathogenesis remain elusive. Hence, it is imperative to investigate the underlying mechanism and develop novel effective targets for the treatment of OS.

Long noncoding RNAs (lncRNAs) are transcripts longer than 200 nucleotides that lack protein-coding capacity.[4-7] An increasing number of studies have indicated that lncRNAs are correlated with tumor occurrence, development, and prognosis.[8] In addition, a lot of researches have explored the role of lncRNAs in OS. It was reported that lncRNA SNHG10 accelerated OS progression via Wnt/β−catenin pathway.[9] A previous study demonstrated that LINC00629 could activate the KLF4/LAMA4 axis, thus leading to a poor prognosis in OS.[10] Furthermore, LINC00324 was found to promote OS development by regulating WDR66.[11] HOXA transcript antisense RNA myeloid-specific 1 (HOTAIRM1) is a novel identified lncRNA that maps within the HOXA gene cluster at human chromosome 7p15.2.[12] Recently, growing evidence has suggested that HOTAIRM1 is an oncogene in multiple cancers and is important in tumorigenesis and development. It has been reported that HOTAIRM1 is upregulated in oral squamous cell carcinoma (OSCC) and enhances OSCC development.[13] HOTAIRM1 is highly expressed in glioblastoma multiforme (GBM) and is closely related to malignancy grade in GBM patients.[14] Ye et al. demonstrated that HOTAIRM1 was involved in ovarian cancer (OV) development by upregulating MMP9 expression.[15] However, the biological function of HOTAIRM1 in OS is unclear.

The mTOR pathway is frequently activated in various diseases.[16] mTOR exerts its biological functions in protein synthesis, cell growth and metabolism mainly through the phosphorylation of two important downstream substrates, 70S6K (ribosomal protein 70S6 kinase) and 4E-BP1, which next phosphorylate effector S6 (ribosomal protein S6).[17-19] Interestingly, growing evidence shows that the mTOR pathway can stimulate tumor progression via the Warburg effect.[17,20,21,22] The Warburg effect is a phenomenon in which virtually all tumor cells consume glucose and produce lactic acid for adenosine triphosphate (ATP) production despite the presence of ample oxygen.[23,24] Nevertheless, the association between mTOR and the Warburg effect in OS remains unclear.

In this study, we revealed that HOTAIRM1 was upregulated in OS and stimulated tumor progression by activating the Warburg effect. Mechanistically, HOTAIRM1 competes with a key regulator of the mTOR pathway, Rheb, for miR-664b-3p, thus resulting in upregulation of Rheb expression, activation of the mTOR pathway, and the transformation from oxidative phosphorylation to aerobic glycolysis. Collectively, the HOTAIRM1-miR-664b-3p/Rheb/mTOR axis may be a novel target for OS therapy.

2 | MATERIALS AND METHODS

2.1 | Cell culture and reagents

The human OS cell lines MG63, U-2OS, MNNG-HOS, and Saos-2 and the human osteoblast cell line hFOB1.19 were acquired from the Cell Bank of the Chinese Academy of Sciences. FTI (farnesyltransferase inhibitor, a Rheb inhibitor) was purchased from Sigma (Sigma, USA). OS cells were incubated at 37°C in humidified air containing 5% carbon dioxide, while hFOB1.19 cells were maintained at 34.5°C with 5% CO2 in a humidified atmosphere. All cells were cultured in a medium that contained 10% fetal bovine serum (FBS) and 1% penicillin–streptomycin.

2.2 | Quantitative RT–PCR (qRT-PCR)

Total RNA was isolated and reverse transcribed to cDNA following the manufacturer's instructions (Vazyme). qRT-PCR analysis was conducted as previously described. β-actin and U6 expression were used for normalization.[25]

2.3 | Cell transfection

The sequences of shRNAs targeting HOTAIRM1 were sh-1, 5′-CTGGAGACTGGTAGCTTATTA-3′ and sh-2, 5′- AGCTGGGAGAT TAATCAACCA-3′. HOTAIRM1 shRNA plasmids and their negative controls were purchased from Gene Pharma. The negative control plasmid and the plasmid containing Rheb-HA were purchased from OBiO Technology. We packaged these plasmids into virus particles using HEK 293 T cells and determined the viral titers. To obtain stable HOTAIRM1-knockdown cell lines or Rheb-overexpressing cell lines, target cells were seeded on six-well plates and coinfected with 1×10^8 lentivirus-transducing units and polybrene (Sigma). After 72 h, the infected cells were screened with 2.5 μg/mL puromycin. The interference efficiency was verified by qRT-PCR and Western blotting.

Control mimics, miR-579-3p mimics, miR-664b-3p mimics, miR-142-5p mimics, miR-5590-3p mimics, control inhibitor, and miR-664b-3p inhibitor, purchased from Gene-Pharma, were transfected into target cells with Lipofectamine 3000 (Invitrogen) according to the supplier's protocol.

2.4 | Western blotting

We used RIPA buffer (Sigma), which contained protease inhibitors (Roche), to extract total protein. Protein samples were electrophoresed on 12% SDS-PAGE gels. After transfer, the membranes were blocked for 1 h with 5% skim milk and then incubated with primary antibodies overnight at 4°C. The membranes were incubated in secondary antibody following washing in TBST. Subsequently,

the membranes were washed again in TBST, and an ECL detection kit (Share-bio) was used to determine luminescence. Densitometric analysis of the Western blotting protein was performed using the ImageJ software.

2.5 | Cell proliferation assay and cell apoptosis assay

Cell-Counting Kit-8 (CCK-8) assay, EdU assay, colony formation assay, and cell apoptosis assay were performed as mentioned previously.[24]

2.6 | Mouse xenograft assay

This experiment was performed following the guidelines of the Research Ethics Committee of East China Normal University. First, male BALB/C nude mice (5–6 weeks old) were randomly divided into several groups ($n=5$ per group). Subsequently, 1.5×10^6 target cells were injected subcutaneously into mice. Tumor volume and weight were detected every 5 days. Finally, all tumors were isolated and measured after mice were euthanized on day 20.

2.7 | Dual-luciferase reporter assay

Dual-luciferase reporter assay was performed to determine the association among HOTAIRM1, miR-664b-3p, and Rheb as previously described.[26]

2.8 | Database analysis

Data from TargetScan (http://www.targetscan.org/) and StarBase (http://starbase.sysu.edu.cn/index.php) were applied to analyze potential interacting genes of miR-664b-3p or HOTAIRM1.

2.9 | Immunohistochemistry staining

Immunohistochemistry (IHC) assay was carried out as previously mentioned.[27] Cell proliferation in xenograft tumor tissues was assessed by corresponding primary antibodies against Ki67 (GB13030; Servicebio) at 1:200 dilutions. The apoptosis of xenograft tumor cells was assayed using a TUNEL kit (Roche) as previously described.[27]

2.10 | Fluorescence in situ hybridization (FISH)

A microarray containing tissue from 40 OS patients was obtained from Alena Biotechnology Co., Ltd. (Xi'an). OS tissue sections were hybridized with HOTAIRM1, miR-664b-3p, and Rheb probes (Servicebio). FISH was performed as reported previously.[24]

2.11 | Bioinformatic analysis and survival analysis

Microarray data from the GSE87624 data set were directly downloaded from GEO (Gene Expression Omnibus) (http://www.ncbi.nlm.nih.gov/geo/) and consisted of 44 disease samples and 3 healthy controls. Samples from two groups were analyzed by limma package in SangerBox (http://sangerbox.com/).[28]

2.12 | Statistical analyses

All statistical results are presented as the means ± SDs. Statistical analyses were conducted using two-tailed Student's *t*-test for comparison of different groups (GraphPad Prism, version 9.3.1 for Windows). A *p*-value of <0.05 was considered to indicate a statistically significant difference.

3 | RESULTS

3.1 | HOTAIRM1 was upregulated in OS cells and tissue

To identify differentially expressed genes in OS, the gene expression profiles of GSE87624 from the GEO database were analyzed using SangerBox. As shown in Figure 1A,B and Table S1, differentially expressed genes between OS and normal tissues were identified using the R package limma (logFC >1 and *p*-value <0.05). Among these differentially expressed genes, we discovered that the lncRNA HOTAIRM1 was significantly upregulated in OS samples compared with normal samples (Figure 1C). To further validate these results, we evaluated the expression level of HOTAIRM1 in tissue samples through FISH using a specific HOTAIRM1 probe on an OS tissue microarray ($n=40$) (Figure 1D). We found that higher HOTAIRM1 expression was closely associated with advanced pathological stage in OS (Figure 1E). Moreover, HOTAIRM1 expression in the normal human osteoblast cell line (hFOB1.19) and in OS cell lines (MG63, U-2OS, MNNG-HOS, and Saos-2) was detected via qRT-PCR. As Figure 1F shows the expression of HOTAIRM1 increased remarkably in OS cell lines (especially U-2OS and MNNG-HOS cells) compared with hFOB1.19 cells. Taken together, the data above confirmed that HOTAIRM1 is upregulated in OS tissues and cells and might be related to the progression of OS.

3.2 | HOTAIRM1 promoted proliferation and inhibited apoptosis in OS cells

To identify the role of lncRNA HOTAIRM1 in OS progression, stable HOTAIRM1-knockdown MNNG-HOS and U-2OS cell lines were constructed to provide additional insight into the biological function of HOTAIRM1 in the development of OS. The knockdown efficiency of HOTAIRM1 was confirmed through qRT-PCR (Figure 2A).

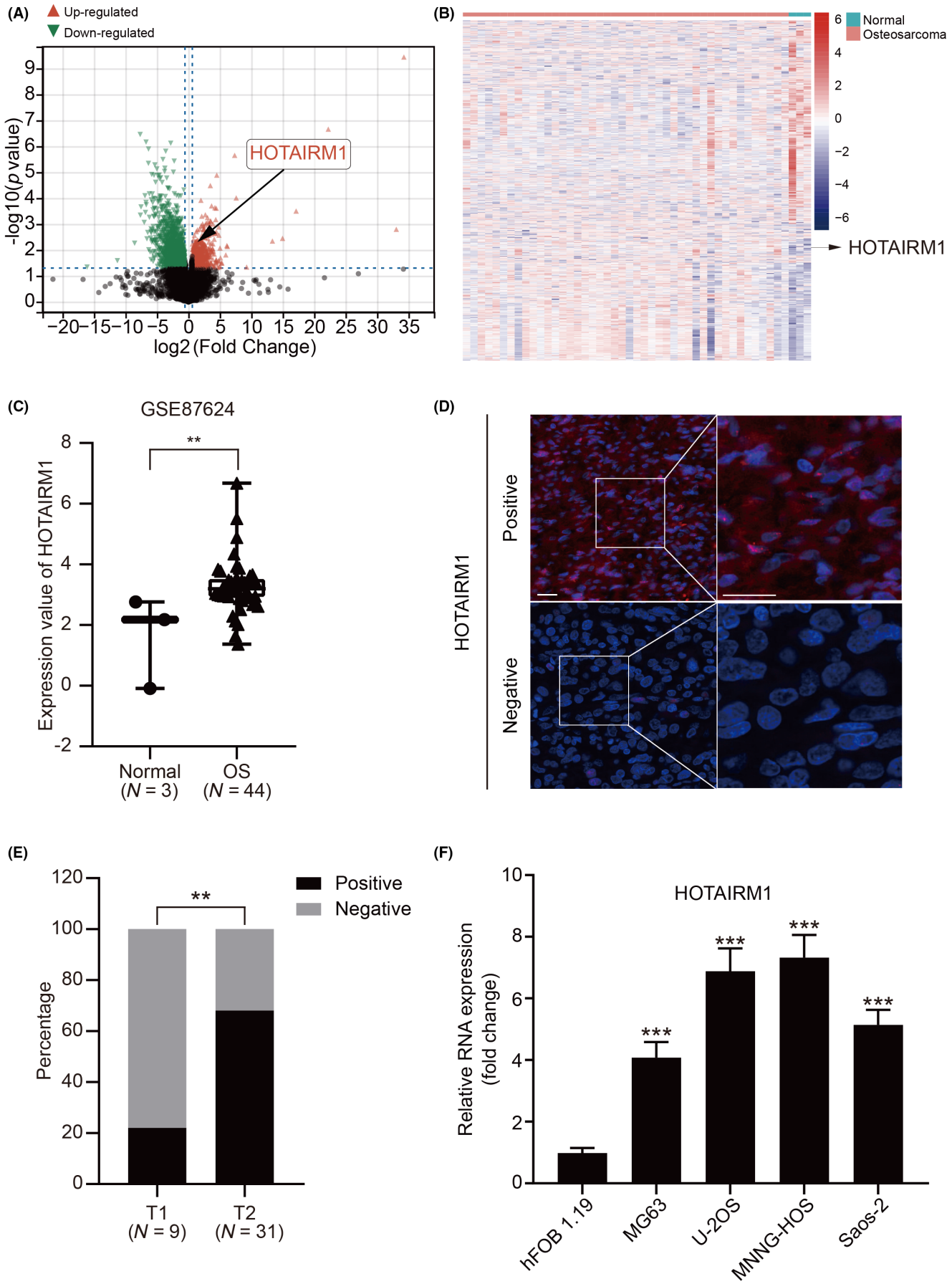
(A)
Up-regulated
Down-regulated
HOTAIRM1
-log10(p value)
log2 (Fold Change)
(B)
Normal
Osteosarcoma
HOTAIRM1
(C)
GSE87624
Expression value of HOTAIRM1
Normal (N = 3)
OS (N = 44)
(D)
HOTAIRM1
Positive
Negative
(E)
Positive
Negative
Percentage
T1 (N = 9)
T2 (N = 31)
(F)
HOTAIRM1
Relative RNA expression (fold change)
hFOB 1.19
MG63
U-2OS
MNNG-HOS
Saos-2

FIGURE 1 HOTAIRM1 was upregulated in osteosarcoma (OS) cells and tissue. (A) Volcano plot representing the differentially expressed genes in GEO datasets (GSE87624). (B) Heatmap showed the differentially expressed genes in GSE87624 downloaded from the GEO database. (C) The expression of HOTAIRM1 in normal and OS samples of the GSE87624 dataset. (D) Representative FISH photographs of the expression patterns of HOTAIRM1 in human OS tissues. Scale bars = 20 μm. (E) Statistical analysis of FISH results based on the expression level of HOTAIRM1 in T1-stage ($n = 9$) and T2-stage ($n = 31$) OS tissues. (F) Relative HOTAIRM1 mRNA levels of MG63, U-2OS, MNNG-HOS, and Saos-2 relative to hFOB1.19 cells were determined using qRT-PCR. Results are displayed as mean ± SD, $^{*}p < 0.05$, $^{**}p < 0.01$, $^{***}p < 0.001$.

As determined by CCK-8 assay, the proliferative capacity of U-2OS and MNNG-HOS cells was significantly inhibited by HOTAIRM1 knockdown (Figure 2B,C). Colony formation assays indicated that HOTAIRM1 knockdown weakened its promoting effect on cell proliferation (Figure 2D,E). The same result was confirmed in the EdU assay (Figure 2F). Furthermore, we found that downregulation of HOTAIRM1 greatly stimulated apoptosis in OS cells compared with that in the control group (Figure 2G,H). Together, our data demonstrated that HOTAIRM1 induced the proliferation and suppressed the apoptosis of OS cells in vitro.

3.3 | Knockdown of HOTAIRM1 inhibits the Warburg effect and the expression of glycolysis-related genes in OS cells

As is well known, the Warburg effect is a hallmark of cancers and contributes to the proliferation of OS.[29,30] To determine whether HOTAIRM1 promotes OS proliferation by contributing to the regulation of aerobic glycolysis, a metabolic flux analyzer was used to measure ECAR, an indicator of glycolytic activity, and OCR, an indicator of oxidative phosphorylation, in HOTAIRM1-knockdown and control OS cells. We found that HOTAIRM1 knockdown resulted in a low level of glycolysis in U-2OS and MNNG-HOS cells (Figure 3A,B) but increased the oxidative phosphorylation capacity in these cells (Figure 3C,D). Moreover, Figure 3E,F suggests that silencing HOTAIRM1 suppressed the formation of lactate and increased the level of ATP production. In general, these findings revealed that HOTAIRM1 knockdown suppresses the Warburg effect in OS cells.

To investigate whether HOTAIRM1 modulated the expression of glycolysis-related genes, qRT-PCR and Western blotting were performed to check their RNA and protein levels. As shown in Figure 3G,H and Figure S1A-F, the expression of these glycolysis-related genes, including GLUT1, HK2, LDHA, and PGK1, was largely inhibited at both the RNA and protein levels in HOTAIRM1-knockdown cells. These findings demonstrated that HOTAIRM1 plays an important role in the modulation of glycolytic metabolism.

3.4 | HOTAIRM1 stimulates OS progression via Rheb/mTOR/c-MYC pathway-mediated glycolysis

There are reports that the mTOR pathway plays an important role in the Warburg effect by regulating the expression of c-MYC, a key regulator of glycolysis.[31-33] On account of the association between the mTOR pathway and the Warburg effect, we sought to explore whether HOTAIRM1 regulates the Warburg effect by activating the mTOR pathway in OS.

Afterward, we used Western blotting to investigate the link between HOTAIRM1 and the mTOR pathway. We found that the expression of AKT, phospho-AKT (p-AKT), and mTOR did not change significantly in HOTAIRM1-knockdown OS cells, while the expression levels of Rheb, phospho-mTOR (p-mTOR), and c-MYC were reduced (Figure S1G). As is known, Rheb interacts with mTOR directly and activates it in the GTP-bound form.[34] According to the association between HOTAIRM1 and the mTOR pathway, we tried to explore whether HOTAIRM1 promotes OS progression by modulating mTOR/c-MYC-mediated glycolysis in a Rheb-dependent manner. Subsequently, we overexpressed Rheb in wild-type (WT) and HOTAIRM1-knockdown OS cell lines and verified the overexpression efficiency through Western blotting. Meanwhile, we found that the expression of p-mTOR, c-MYC, and the genes involved in glycolysis, including GLUT1, HK2, and LDHA, were partly rescued by Rheb overexpression (Figure 4A and Figure S2A–G). As shown in Figure 4B–D and Figure S2H, overexpression of Rheb promoted cell proliferation in HOTAIRM1-knockdown cells. The results of the apoptosis assay indicated that overexpression of Rheb partly reversed the enhancing effects of HOTAIRM1 knockdown on apoptosis in U-2OS and MNNG-HOS cells (Figure 4E and Figure S2I). Moreover, the Warburg effect was partially restored by overexpressing Rheb in OS cells (Figure 4F–I). In general, these findings revealed that HOTAIRM1 modulated Rheb/mTOR/c-MYC-mediated glycolysis and then contributed to the growth of OS.

3.5 | miR-664b-3p directly targets Rheb in OS cells

As mentioned, Rheb expression is regulated by HOTAIRM1. However, no direct binding site between HOTAIRM1 and Rheb was predicted by online prediction algorithms. It has been reported that lncRNAs can modulate the expression of target genes in various cell processes by acting as miRNA sponges. Therefore, we assumed that HOTAIRM1 modulates Rheb expression via microRNAs. Next, we identified four potential microRNAs that target Rheb and are regulated by HOTAIRM1 using two prediction algorithms, TargetScan and StarBase (Figure 5A). These four miRNAs were overexpressed in U-2OS and MNNG-HOS cells, and the overexpression efficiency was detected via qRT–PCR (Figure S3A,B). Subsequently, we found that the RNA expression of Rheb decreased significantly in U-2OS and MNNG-HOS cells

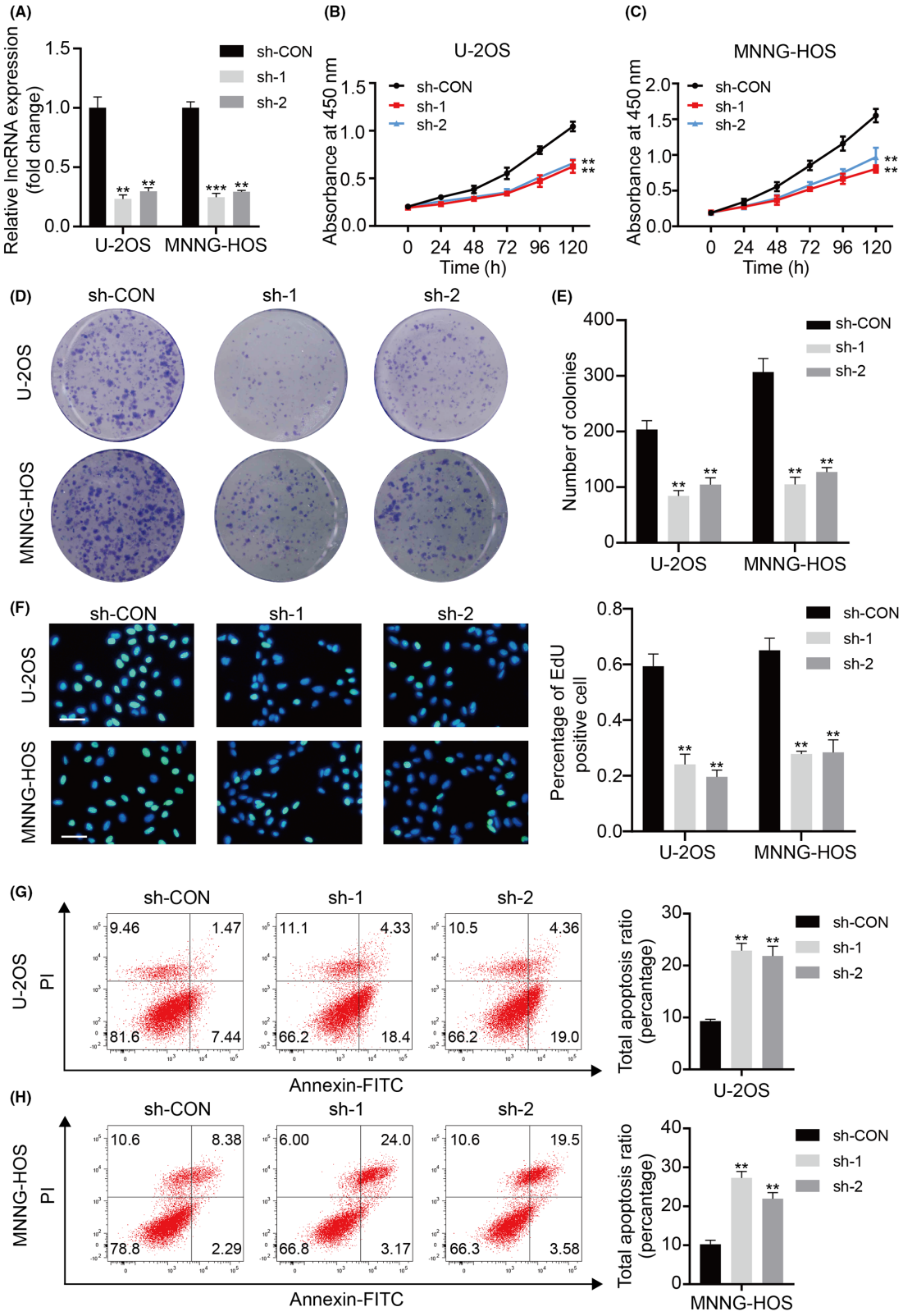

FIGURE 2 HOTAIRM1 promoted proliferation and inhibited apoptosis in osteosarcoma (OS) cells. (A) Interference efficacy of sh-RNA targeting of HOTAIRM1 in U-2OS and MNNG-HOS cells was determined by qRT-PCR. (B, C) Knockdown of HOTAIRM1 suppressed the proliferation capability of U-2OS and MNNG-HOS cells using CCK-8 assay. (D, E) Knockdown of HOTAIRM1 suppressed the proliferation of OS cells (U-2OS and MNNG-HOS) using colony formation assay. (F) HOTAIRM1 shRNA decreased the percentage of EdU-positive OS cells. Representative photographs of the EdU incorporation assay are shown in the left panel; scale bars = 20 μm. (G, H) The knockdown of HOTAIRM1 significantly induces apoptosis of U-2OS and MNNG-HOS cells. Results are displayed as mean ± SD. $^{*}p < 0.05$, $^{**}p < 0.01$, $^{***}p < 0.001$.

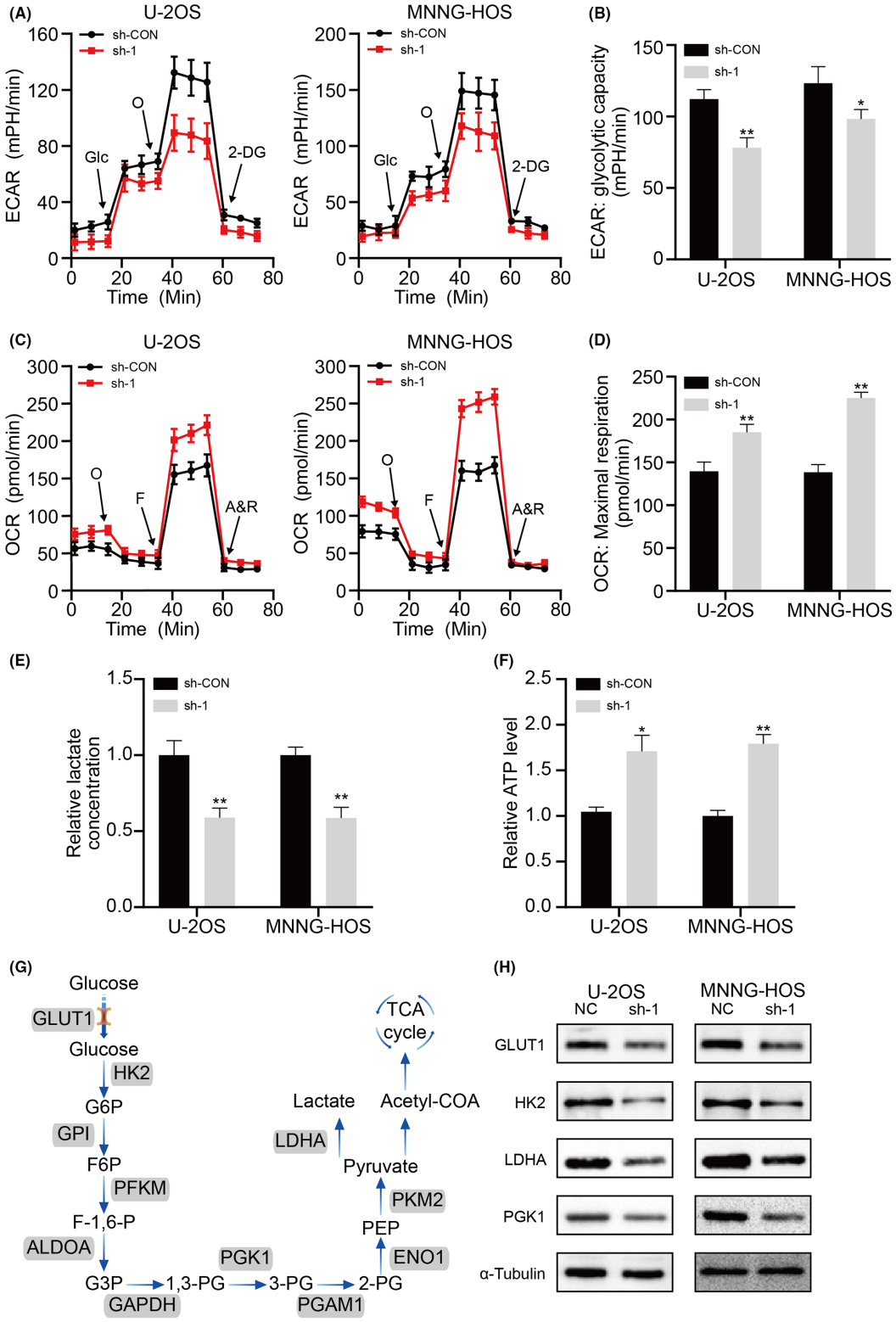

FIGURE 3 Knockdown of HOTAIRM1 inhibits the Warburg effect and the expression of glycolysis-related genes in osteosarcoma (OS) cells. (A) Extracellular acidification rate (ECAR) of U-2OS or MNNG-HOS cells in the sh-Control and sh-HOTAIRM1 group was detected via a Seahorse Bioscience XFp analyzer. Glc, glucose; O, oligomycin; 2-DG, 2-deoxy-d-glucose. (B) Quantification of glycolytic capacity from (A). (C) Oxygen consumption rates (OCR) of U-2OS or MNNG-HOS cells in the sh-Control and sh-HOTAIRM1 group was detected using a Seahorse Bioscience XFp analyzer. O, oligomycin; F, FCCP; A&R, antimycin A/rotenone. (D) Quantification of maximal respiration from (C). (E) Lactate production was determined in different groups (sh-Control and sh-HOTAIRM1). (F) Adenosine triphosphate (ATP) level was determined in different groups (sh-Control and sh-HOTAIRM1). (G) Schematic diagram of the aerobic glycolysis pathway. (H) Protein levels of aerobic glycolysis enzymes following knockdown of HOTAIRM1. Results are displayed as mean ± SD, $^{*}p < 0.05$, $^{**}p < 0.01$, $^{***}p < 0.001$.

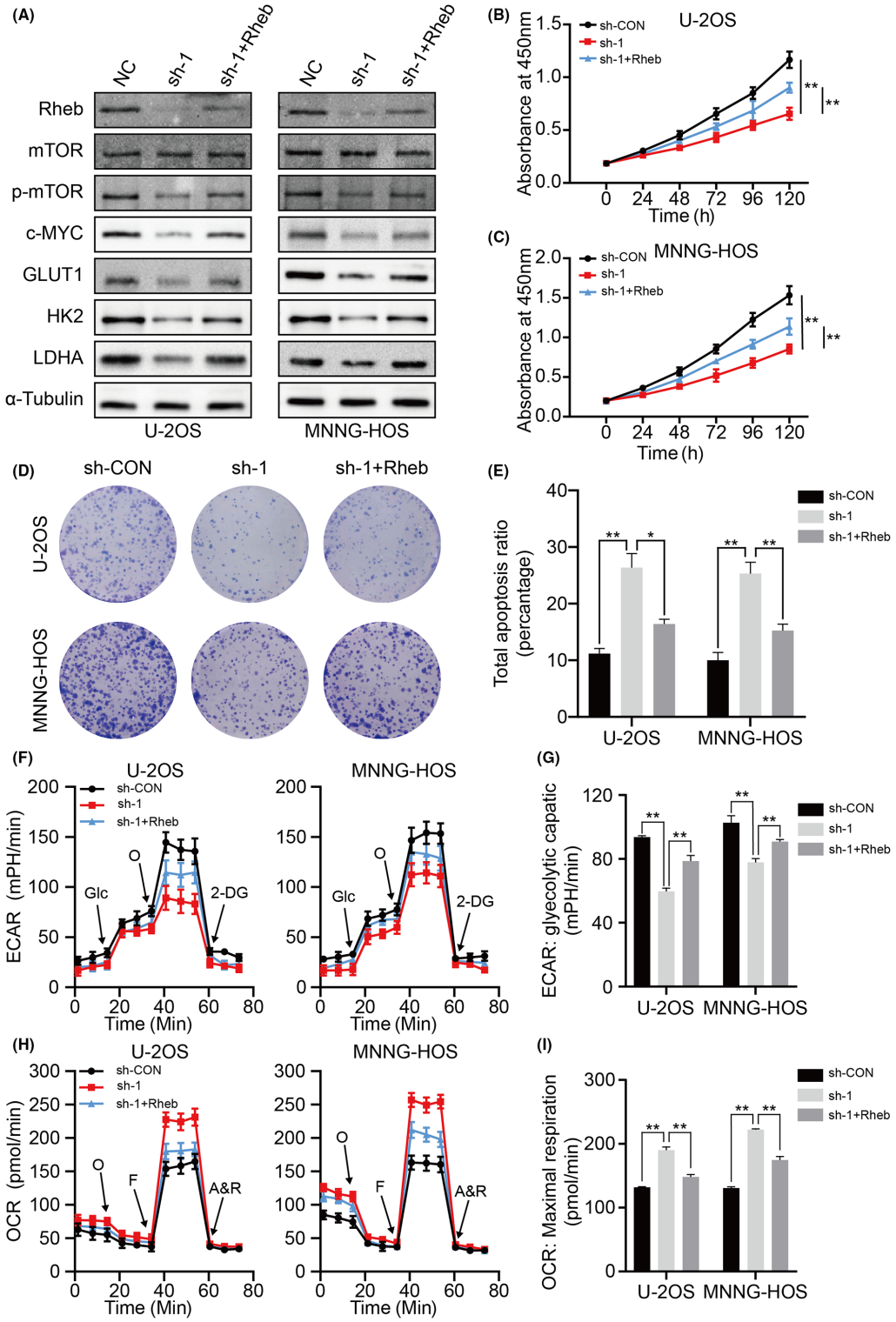

FIGURE 4 HOTAIRM1 stimulates osteosarcoma (OS) progression via Rheb/mTOR/c-MYC pathway-mediated glycolysis. (A) Protein levels of Rheb, total and phosphorylated mTOR, c-Myc, and aerobic glycolysis enzymes following overexpression of Rheb in HOTAIRM1-knockdown cells. B, C, Overexpression of Rheb partly reversed the suppressed effects of HOTAIRM1 knockdown on the cell viability of U-2OS and MNNG-HOS cells using CCK-8 assay. (D) Overexpression of Rheb partly reversed the suppressed effects of HOTAIRM1 knockdown on the colony-formation capability of U-2OS and MNNG-HOS cells. (E) Overexpression of Rheb partly reversed the induced effect of HOTAIRM1 knockdown on the apoptosis of OS cells (U-2OS and MNNG-HOS). (F) Extracellular acidification rates (ECARs) in OS cells (U-2OS and MNNG-HOS) in different groups (sh-Control, sh-HOTAIRM1, and sh-HOTAIRM1 + ov-Rheb) were determined. (G) Quantification of the glycolytic capacity from F. (H) Oxygen consumption rates (OCR) in OS cells (U-2OS and MNNG-HOS) in different groups (sh-Control, sh-HOTAIRM1, and sh-HOTAIRM1 + ov-Rheb) were determined. (I) Quantification of maximal respiration from (H). Results are displayed as mean ± SD. $^{*}p < 0.05$, $^{**}p < 0.01$, $^{***}p < 0.001$.

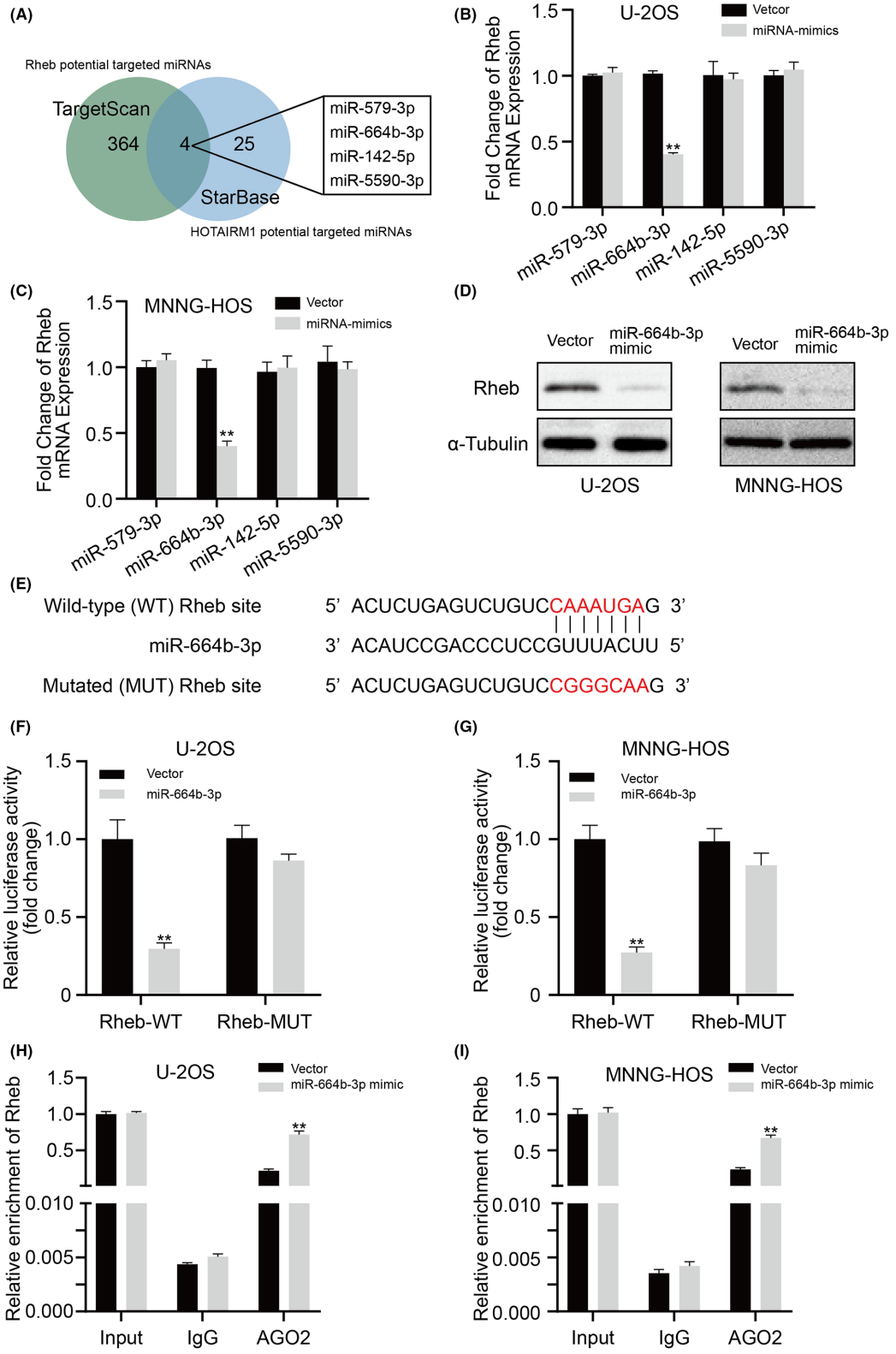

FIGURE 5 miR-664b-3p directly targets Rheb in osteosarcoma (OS) cells. (A) Venn diagram showing the predicted target miRNAs of Rheb and HOTAIRM1 from databases (TargetScan and StarBase). (B, C) The mRNA expression patterns of Rheb in predicted target miRNA mimics the treated or Control U-2OS and MNNG-HOS cells. (D) Western blot showed Rheb expression in U-2OS and MNNG-HOS cells transfected with miR-664b-3p mimics or negative control. (E) Wild-type and mutated sequences of the Rheb mRNA 3'-UTR (mutation site: red). (F, G) The luciferase activity of OS cells (U-2OS and MNNG-HOS) in luciferase reporter plasmid containing wild-type Rheb 3'-UTR (Rheb-WT) and mutant Rheb 3'-UTR (Rheb-MUT) cotransfected with miR-664b-3p mimics or negative control was assessed. (H, I) RIP assays using antibodies against AGO2 or IgG were performed in cellular lysates from U-2OS and MNNG-HOS cells. qRT-PCR showed the relative enrichment of Rheb in cells transfected with miR-664b-3p or NC mimics. Results are displayed as mean ± SD. $^{*}p < 0.05$, $^{**}p < 0.01$, $^{***}p < 0.001$.

due to overexpression of miR-664b-3p (Figure 5B,C). Furthermore, we found that the expression of Rheb at the protein level was reduced in the miR-664b-3p overexpression group. (Figure 5D and Figure S3C). The potential target site of miR-664b-3p on Rheb is shown in Figure 5E. To test the association between miR-664b-3p and Rheb, we performed double luciferase reporter assays. As expected, the miR-664b-3p mimic induced a marked reduction in the luciferase intensity of the WT Rheb 3′UTR (Rheb-WT) reporter, which was not observed in the mutated type (MUT) 3′UTR of the Rheb reporter in OS cells (Figure 5F,G). Additionally, the results of the RNA immunoprecipitation (RIP) assay demonstrated a much higher enrichment level of Rheb in the anti-Argonaute2 (Ago2) group with the overexpression of miR-664b-3p (Figure 5H,I). These data suggested that miR-664b-3p inhibited Rheb expression by interacting with its 3′UTR directly.

3.6 | HOTAIRM1 directly interacts with mir-664b-3p as a sponge in OS

To explore the interaction between HOTAIRM1 and miR-664b-3p in OS cells in depth, we first examined miR-664b-3p expression by qRT-PCR in HOTAIRM1 knockdown and control OS cells, and the results showed that miR-664b-3p expression increased significantly after HOTAIRM1 knockdown (Figure 6A). Next, using StarBase analysis, we discovered that there was a potential binding site between HOTAIRM1 and miR-664b-3p (Figure 6B). In the meantime, the plasmids containing either the WT or MUT miR-664b-3p binding site of the HOTAIRM1 transcript combined with an MS2 binding site were constructed and cotransfected into U-2OS or MNNG-HOS cell lines with a construct containing MS2-binding protein (MS2bp) and GFP. The results of the MS2-based RIP assay demonstrated that miR-664b-3p was largely enriched in RNAs retrieved from the WT MS2bs-HOTAIRM1 group relative to the MUT MS2bs-HOTAIRM1 group (Figure 6C). Moreover, an RNA pulldown assay was performed in OS cells and indicated that miR-664b-3p bound biotin-labeled WT HOTAIRM1 but not MUT HOTAIRM1 (Figure 6D). As revealed in Figure 6E,F, transiently expressing miR-664b-3p induced a marked reduction in the luciferase intensity of HOTAIRM1-WT, which was not observed in the HOTAIRM1-MUT group. Additionally, anti-Ago2 RIP demonstrated the enrichment of endogenous HOTAIRM1 was increased due to miR-664b-3p overexpression in OS cells (Figure 6G,H). Collectively, these results suggested that HOTAIRM1 acts as a sponge for miR-664b-3p via the ceRNA mechanism in OS cells.

3.7 | The inhibitory effect of OS cells triggered by silencing HOTAIRM1 was reversed by miR-664b-3p knockdown

To further assess whether HOTAIRM1 is involved in OS progression through miR-664b-3p, a rescue experiment was conducted with U-2OS and MNNG-HOS cells. We transfected OS cells using sh-HOTAIRM1 plus miR-664b-3p inhibitors. As shown in Figure 7A and Figure S4A–G, silencing HOTAIRM1 significantly inhibited the expression of Rheb, p-mTOR, and glycolysis-related genes at the protein level, which was partly reversed by inhibition of miR-664b-3p. Additionally, we found that silencing HOTAIRM1 markedly suppressed the proliferation of OS cells, while miR-664b-3p knockdown partially reversed this inhibitory effect (Figure 7B–D and Figure S4A). Moreover, the results of the apoptosis assay indicated that the enhancement of apoptosis was partly rescued in the HOTAIRM1-knockdown group with the inhibition of miR-664b-3p (Figure 7E and Figure S4B,C). Similarly, miR-664b-3p knockdown partially inhibited the effect of silencing HOTAIRM1 on the Warburg effect (Figure 7F,G). Subsequently, we performed cell proliferation assays in combination with FTI, a Rheb inhibitor. The results of CCK–8 assay indicated that FTI partly reversed the enhancement of miR–664b–3p knockdown on cell proliferation (Figure S5A,B). Meanwhile, the colony formation capacity of OS was remarkablely supressed due to the application of FTI (Figure S5C,D). In conclusion, these findings collectively indicated that HOTAIRM1 works as a critical promotor of OS growth and aerobic glycolysis by the miR-664b-3p/Rheb axis.

3.8 | HOTAIRM1 knockdown attenuates OS growth via the miR-664b-3p/Rheb axis in vivo

Next, to further confirm whether HOTAIRM1 promotes OS cell proliferation in vivo, xenograft models of OS were established in nude mice by subcutaneous injections in established stable MNNG-HOS cell lines. As depicted in Figure 8A,B and Figure S6A, compared with the control conditions, HOTAIRM1 knockdown reduced the tumor burden markedly and inhibited the growth of

FIGURE 6 HOTAIRM1 directly interacts with mir-664b-3p as a sponge in osteosarcoma (OS). (A) The expression of miR-664b-3p was upregulated in U-2OS and MNNG-HOS transfected with HOTAIRM1 shRNA or the control shRNA by RT-qPCR. (B) Wild-type and the mutated sequences of HOTAIRM1 mRNA 3'-UTR (mutation site: red). (C) Top panel shows a schematic image of a construction containing HOTAIRM1 wild type combined with MS2 binding sequence. MS2-RIP followed by miR-664b-3p qRT-PCR to measure miR-664b-3p endogenously associated with HOTAIRM1. (D) U-2OS and MNNG-HOS cells lysates were incubated with biotin-labeled HOTAIRM1. qRT-PCR measured miR-664b-3p expression in the products of pulldown by biotin. (E, F) Luciferase activity of OS cells (U-2OS and MNNG-HOS) in luciferase reporter plasmid containing wild-type HOTAIRM1 3'-UTR (HOTAIRM1-WT) and mutant HOTAIRM1 3'-UTR (HOTAIRM1-MUT) cotransfected with miR-664b-3p mimics or negative control was assessed. (G, H) AGO2-RIP followed by qPCR to evaluate HOTAIRM1 level after miR-664b-3p overexpression. Results are displayed as mean ± SD. $^{*}p < 0.05$, $^{**}p < 0.01$, $^{***}p < 0.001$.

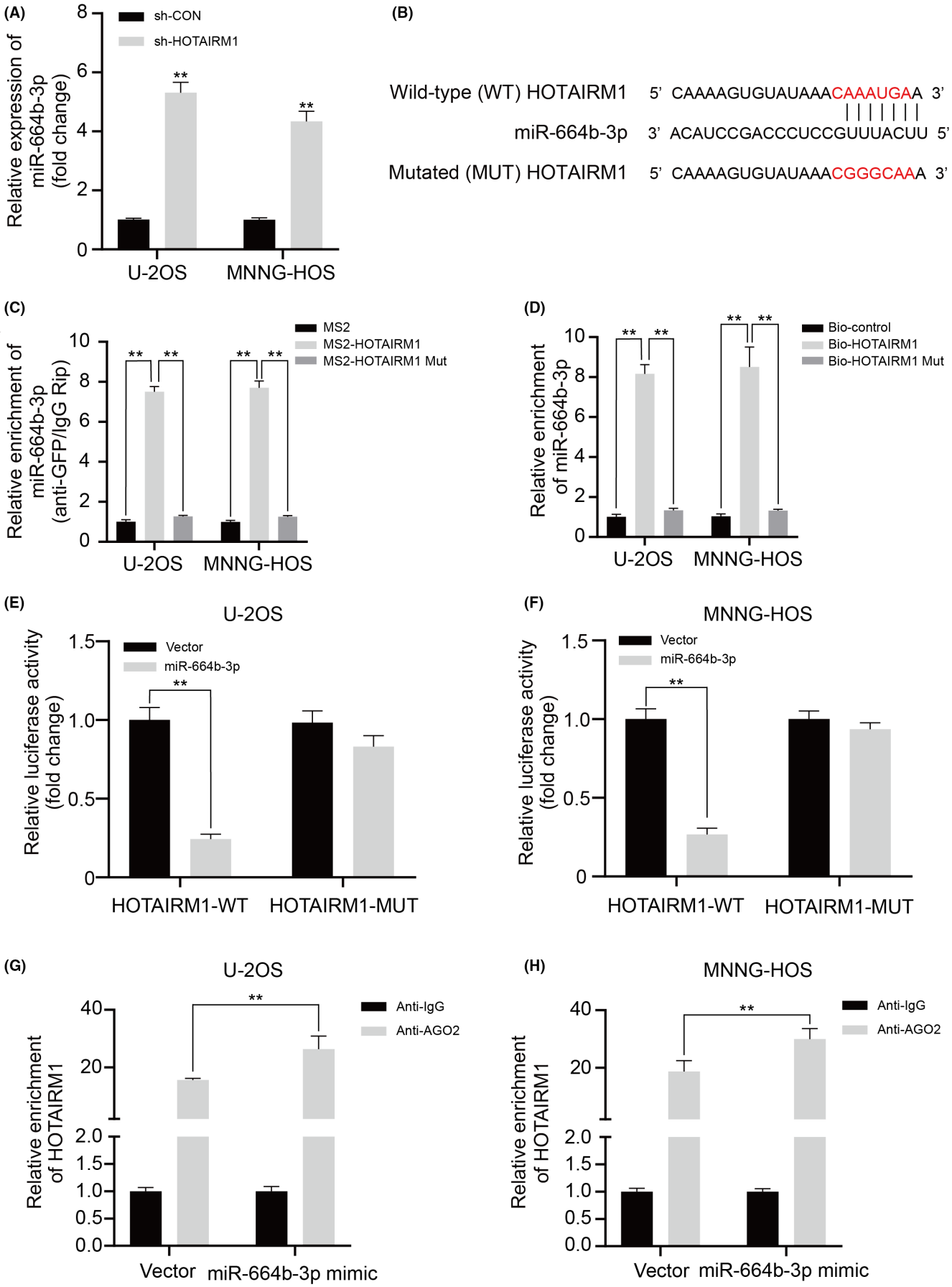
(A)
sh-CON
sh-HOTAIRM1
Relative expression of miR-664b-3p (fold change)
U-2OS
MNNG-HOS
(B)
Wild-type (WT) HOTAIRM1 5' CAAAAGUGUAUAAACAAAUGAA 3'
miR-664b-3p 3' ACAUCCGACCCUCCGUUUACUU 5'
Mutated (MUT) HOTAIRM1 5' CAAAAGUGUAUAAACGGGCAAA 3'
(C)
MS2
MS2-HOTAIRM1
MS2-HOTAIRM1 Mut
Relative enrichment of miR-664b-3p (anti-GFP/IgG Rip)
U-2OS
MNNG-HOS
(D)
Bio-control
Bio-HOTAIRM1
Bio-HOTAIRM1 Mut
Relative enrichment of miR-664b-3p
U-2OS
MNNG-HOS
(E)
U-2OS
Vector
miR-664b-3p
Relative luciferase activity (fold change)
HOTAIRM1-WT
HOTAIRM1-MUT
(F)
MNNG-HOS
Vector
miR-664b-3p
Relative luciferase activity (fold change)
HOTAIRM1-WT
HOTAIRM1-MUT
(G)
U-2OS
Anti-IgG
Anti-AGO2
Relative enrichment of HOTAIRM1
Vector
miR-664b-3p mimic
(H)
MNNG-HOS
Anti-IgG
Anti-AGO2
Relative enrichment of HOTAIRM1
Vector
miR-664b-3p mimic

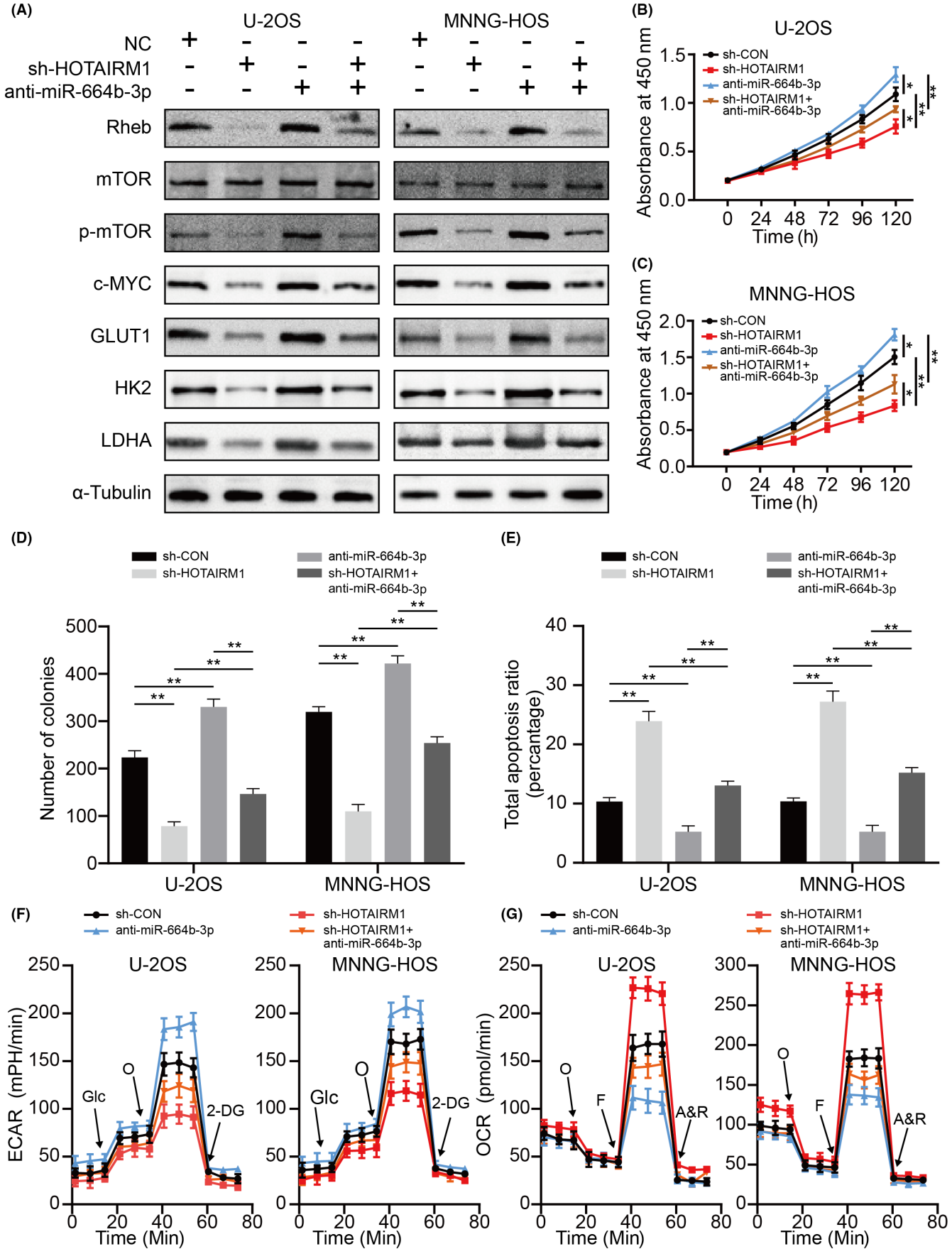
(A)
U-2OS
MNNG-HOS
NC
sh-HOTAIRM1
anti-miR-664b-3p
Rheb
mTOR
p-mTOR
c-MYC
GLUT1
HK2
LDHA
α-Tubulin
(B)
U-2OS
sh-CON
sh-HOTAIRM1
anti-miR-664b-3p
sh-HOTAIRM1+ anti-miR-664b-3p
Absorbance at 450 nm
Time (h)
(C)
MNNG-HOS
(D)
Number of colonies
(E)
Total apoptosis ratio (percantage)
(F)
ECAR (mPH/min)
Glc
O
2-DG
Time (Min)
(G)
OCR (pmol/min)
F
A&R

FIGURE 7 The inhibitory effect of osteosarcoma (OS) cells triggered by HOTAIRM1 knockdown was reversed by miR-664b-3p knockdown. (A) Protein levels of Rheb, total and phosphorylated mTOR, c-Myc, and aerobic glycolysis enzymes in U-2OS and MNNG-HOS cells transfected with miR-664b-3p inhibitor, sh-HOTAIRM1, or negative control. B, C, miR-664b-3p knockdown partly reversed the suppressed effects of HOTAIRM1 knockdown on the cell viability of U-2OS and MNNG-HOS cells using CCK-8 assay. (D) miR-664b-3p knockdown partly reversed the suppressed effects of HOTAIRM1 knockdown on the colony-formation capability of U-2OS and MNNG-HOS cells. (E) miR-664b-3p knockdown partly reversed the induced effect of HOTAIRM1 knockdown on the apoptosis of OS cells (U-2OS and MNNG-HOS). (F) Altered levels of extracellular acidification rate (ECAR) in OS cells (U-2OS or MNNG-HOS) in different groups (sh-Control, sh-HOTAIRM1, sh-HOTAIRM1 + anti-miR-664b-3p and anti-miR-664b-3p). (G) Altered levels of Oxygen consumption rates (OCR) in OS cells (U-2OS or MNNG-HOS) in different groups (sh-Control, sh-HOTAIRM1, sh-HOTAIRM1 + anti-miR-664b-3p and anti-miR-664b-3p). Results are displayed as mean ± SD. $^{*}p < 0.05$, $^{**}p < 0.01$, $^{***}p < 0.001$.

xenograft tumors. Nevertheless, the tumor-promoting effect of HOTAIRM1 was partially rescued by inhibition of miR-664b-3p. Subsequently, the proliferation and apoptosis of cells in xenograft tumors were analyzed by Ki67 staining and TUNEL assay, respectively. As seen in Figure 8C,D, HOTAIRM1 knockdown caused a substantial drop in cell proliferation and induced apoptosis in vivo, while knockdown of miR-664b-3p partially restored this effect. The expression patterns of the HOTAIRM1/miR-664b-3p/Rheb axis were established using FISH and IF staining in xenograft tumors (Figure 8E). This result was further verified in human OS samples (Figure 8F). A positive association between the expression pattern of HOTAIRM1 and Rheb and a negative association between HOTAIRM1 and miR-664b-3p, as well as miR-664b-3p and Rheb were apparent (Figure 8G–I). Therefore, these data indicated that lncRNA HOTAIRM1 stimulates OS cell growth through the miR-664b-3p/Rheb axis in vivo.

4 | DISCUSSION

Accumulating studies have reported that aberrantly expressed lncRNAs exert important functions in various human diseases, including OS, by regulating downstream gene expression. A previous study reported that lncRNA MELTF-AS1 increased the ability of OS to metastasize through the miR-485-5p/MMP14 axis.[35] Shi et al. revealed that highly expressed AFAP1-AS1 plays an oncogenic role by activating the RhoC/ROCK1/p38MAPK/Twist1 signaling pathway in OS.[36] HOTAIRM1, which was first discovered in promyelocytic leukemia cells, has been reported to be upregulated and lead to poor prognosis in various cancers.[12] In our study, we found that HOTAIRM1 was highly expressed in OS cells and tissues. Furthermore, HOTAIRM1 facilitated the proliferation while suppressing the apoptosis of OS cells in vivo and in vitro.

Recently, the competing endogenous RNA (ceRNA) hypothesis, which suggests that lncRNAs modulate mRNA expression by working as miRNA sponges, has received increasing attention.[37] Emerging evidence indicates that HOTAIRM1 can also act as a ceRNA.[38,39] In our study, we found that HOTAIRM1 promoted OS cell proliferation and inhibited OS cell apoptosis by modulating the miR-664b-3p/Rheb pathway.

Rheb, which belongs to the small GTPase superfamily, performs its function by activating the mTOR signaling pathway in its GTP-bound form.[40,41] Growing evidence indicates that the Rheb/mTOR pathway critically affects cell proliferation, apoptosis, metabolism, tumorigenesis, and development.[42-45] Dong et al. suggested that VEPH1 downregulation promoted hepatocellular carcinoma (HCC) cell proliferation, migration, and invasion by activating Rheb/mTOR signaling.[46] In breast cancer, Rheb contributes largely to E2-induced proliferation as a regulator of the mTOR pathway.[47] Our study demonstrated that Rheb is upregulated by HOTAIRM1, which functions as a ceRNA by sponging miR-664b-3p and accelerates the progression of OS via the mTOR pathway.

The Warburg effect is a characteristic of rapidly proliferating cells.[48] mTOR signaling, which is an irreplaceable activator in various fundamental cellular processes, including metabolism, is known to be one of many glycolysis-related pathways.[49,50] It was reported that mTOR stimulated glycolysis in a c-MYC-dependent manner.[51] C-MYC, which functions as a classical regulator of cell metabolism, mediates glucose metabolism reprogramming by targeting glycolytic enzymes.[30,52] Herein, our results confirmed that HOTAIRM1 activates the Warburg effect in the Rheb/mTOR/c-MYC pathway.

In conclusion, our findings revealed that HOTAIRM1, whose expression is increased in OS, functions by sponging miR-664b-3p to enhance Rheb expression, thereby contributing to the growth of OS via mTOR pathway-mediated glucose metabolism reprogramming. These data highlight that HOTAIRM1 may be a potential molecular target for OS therapy.

ACKNOWLEDGMENTS

We thank Ruikai Zhou and Dr. Yunkun Zhang (Department of Orthopedics, The Affiliated Changzhou Second People's Hospital of Nanjing Medical University, Changzhou Medical Center, Nanjing Medical University, Changzhou) for technical assistance.

FUNDING INFORMATION

This study was supported by the National Science Foundation of China (NSFC) (Grant No. 82160555), Natural Science Foundation of Xinjiang Uygur Autonomous Region (2022D01A317), and the Changzhou Medical Center Project (CMCB202208).

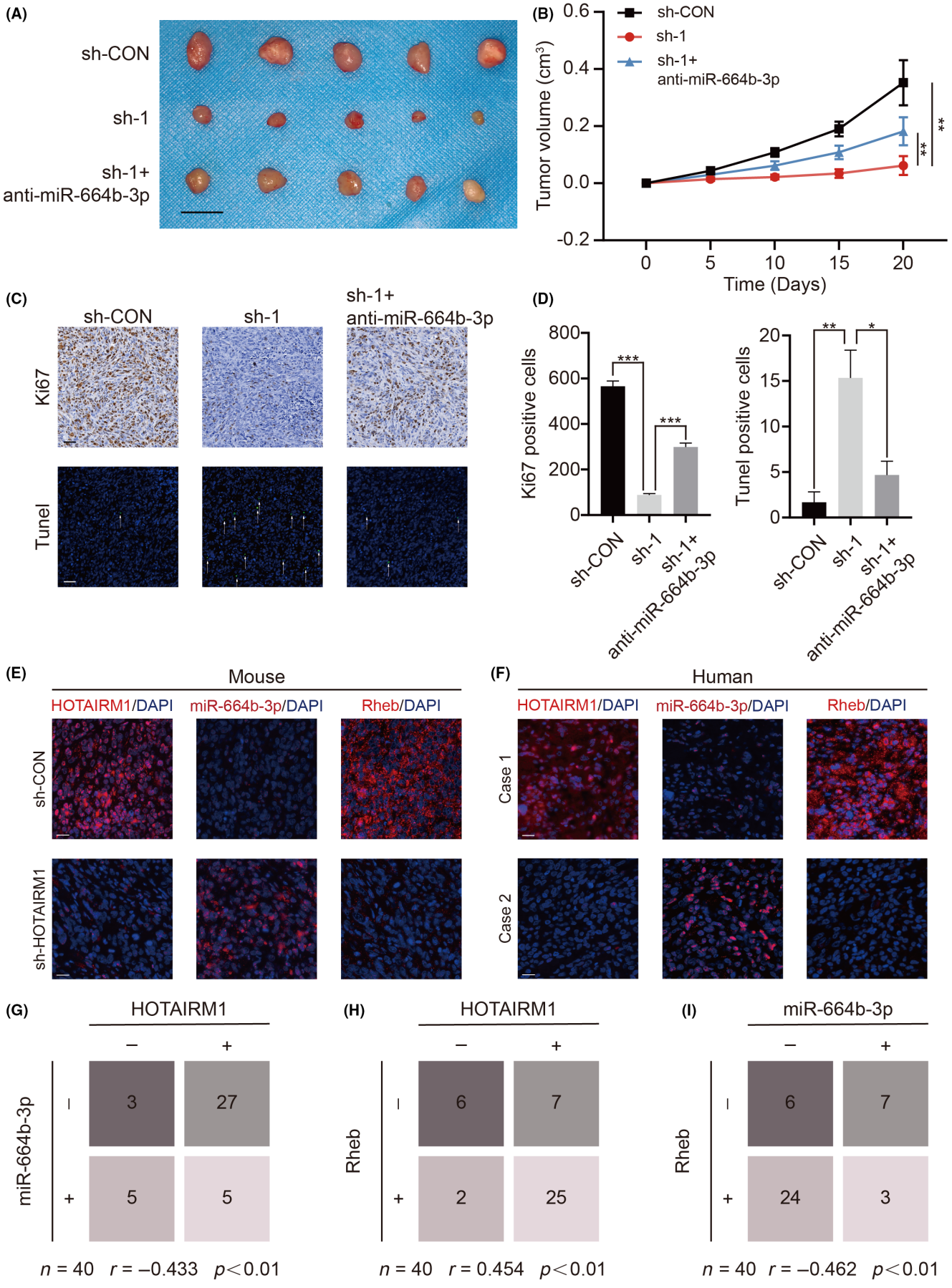
(A)
sh-CON
sh-1
sh-1+
anti-miR-664b-3p
(B)
sh-CON
sh-1
sh-1+
anti-miR-664b-3p
Tumor volume (cm3)
0.6
0.4
0.2
0.0
-0.2
0
5
10
15
20
Time (Days)
**
**
(C)
sh-CON
sh-1
sh-1+
anti-miR-664b-3p
Ki67
Tunel
(D)
Ki67 positive cells
800
600
400
200
0
***
***
sh-CON
sh-1
sh-1+
anti-miR-664b-3p
Tunel positive cells
20
15
10
5
0
**
*
sh-CON
sh-1
sh-1+
anti-miR-664b-3p
(E)
Mouse
HOTAIRM1/DAPI
miR-664b-3p/DAPI
Rheb/DAPI
sh-CON
sh-HOTAIRM1
(F)
Human
HOTAIRM1/DAPI
miR-664b-3p/DAPI
Rheb/DAPI
Case 1
Case 2
(G)
HOTAIRM1
–
+
miR-664b-3p
–
+
3
27
5
5
n = 40 r = –0.433 p<0.01
(H)
HOTAIRM1
–
+
Rheb
–
+
6
7
2
25
n = 40 r = 0.454 p<0.01
(I)
miR-664b-3p
–
+
Rheb
–
+
6
7
24
3
n = 40 r = –0.462 p<0.01

FIGURE 8 HOTAIRM1 knockdown attenuates osteosarcoma (OS) growth via the miR-664b-3p/Rheb axis in vivo. (A) Morphologic characteristics of xenograft tumors from different groups (sh-Control, sh-HOTAIRM1, sh-HOTAIRM1 + anti-miR-664b-3p) ($n = 5$). Scale bars = 1 cm. (B) Knockdown of miR-664b-3p partly reversed the attenuation of tumor rates that were induced by HOTAIRM1 knockdown. Tumors were measured every fifth day. (C) Representative images of Ki67 and TUNEL staining in the xenograft tumors from each experimental group of nude mice. A TUNEL positive cell is indicated with an arrow. Scale bars = 50 μm. (D) Quantification of positive cells from (C). (E) Representative photographs of the expression patterns of HOTAIRM1, miR-664b-3p, and Rheb in tumor tissues from subcutaneous xenograft mouse model by immunofluorescence (IF) and FISH. Scale bars = 20 μm. (F) Representative photographs of the expression patterns of HOTAIRM1, miR-664b-3p, and Rheb in human OS tissues by IF and FISH. Scale bars = 20 μm. (G) Negative correlation between the expression patterns of HOTAIRM1 and miR-664b-3p ($n = 40$, $r = -0.433$, $p < 0.01$). (H) Positive correlation between the expression patterns of HOTAIRM1 and Rheb ($n = 40$, $r = 0.454$, $p < 0.01$). (I) Negative correlation between the expression patterns of miR-664b-3p and Rheb ($n = 40$, $R = -0.462$, $p < 0.01$). Results are displayed as mean ± SD. $^{*}p < 0.05$, $^{**}p < 0.01$, $^{***}p < 0.001$.

CONFLICT OF INTEREST STATEMENT

The authors declare that they have no conflict of interest.

ETHICS STATEMENTS

This study was approved by the research medical ethics committee of the Affiliated Hospital of the Nanjing Medical University Animal Protection and Use Committee.

Informed Consent: N/A.

Registry and the Registration No. of the study/trial: N/A.

Animal Studies: N/A.

ORCID

Dong Zhou https://orcid.org/0000-0001-9514-3116
Yifei Shen https://orcid.org/0000-0002-1401-7183

REFERENCES

1. Lu J, Song G, Tang Q, et al. IRX1 hypomethylation promotes osteosarcoma metastasis via induction of CXCL14/NF-kappaB signaling. *J Clin Invest*. 2015;125(5):1839-1856.
2. Whelan J, McTiernan A, Cooper N, et al. Incidence and survival of malignant bone sarcomas in England 1979-2007. *Int J Cancer*. 2012;131(4):E508-E517.
3. Morrow JJ, Bayles I, Funnell APW, et al. Corrigendum: positively selected enhancer elements endow osteosarcoma cells with metastatic competence. *Nat Med*. 2018;24(4):525.
4. Ni W, Yao S, Zhou Y, et al. Long noncoding RNA GAS5 inhibits progression of colorectal cancer by interacting with and triggering YAP phosphorylation and degradation and is negatively regulated by the m(6)a reader YTHDF3. *Mol Cancer*. 2019;18(1):143.
5. Li J, Chen Z, Tian L, et al. LncRNA profile study reveals a three-lncRNA signature associated with the survival of patients with oesophageal squamous cell carcinoma. *Gut*. 2014;63(11):1700-1710.
6. Alvarez-Dominguez JR, Hu W, Yuan B, et al. Global discovery of erythroid long noncoding RNAs reveals novel regulators of red cell maturation. *Blood*. 2014;123(4):570-581.
7. Li J, Hao Y, Mao W, et al. LincK contributes to breast tumorigenesis by promoting proliferation and epithelial-to-mesenchymal transition. *J Hematol Oncol*. 2019;12(1):19.
8. Xu P, Xiao H, Yang Q, et al. The USP21/YY1/SNHG16 axis contributes to tumor proliferation, migration, and invasion of non-small-cell lung cancer. *Exp Mol Med*. 2020;52(1):41-55.
9. Zhu, S, Liu, Y, Wang, X, et al. lncRNA SNHG10 Promotes the Proliferation and Invasion of Osteosarcoma via Wnt/β–Catenin Signaling. *Molecular Therapy – Nucleic Acids*. 2020;22:957-970.
10. Wang, Y, Zheng, S, Han, J, et al. LINC00629 protects osteosarcoma cell from ER stress–induced apoptosis and facilitates tumour progression by elevating KLF4 stability. *Journal of Experimental & Clinical Cancer Research*. 2022;41(1).
11. Wu, S, Gu, Z, Wu, Y, et al. LINC00324 accelerates the proliferation and migration of osteosarcoma through regulating WDR66. *Journal of Cellular Physiology*. 2019;235(1):339–348.
12. Jing Y, Jiang X, Lei L, et al. Mutant NPM1-regulated lncRNA HOTAIRM1 promotes leukemia cell autophagy and proliferation by targeting EGR1 and ULK3. *J Exp Clin Cancer Res*. 2021;40(1):312.
13. Yu, Y, Niu, J, Zhang, X, et al. Identification and Validation of HOTAIRM1 as a Novel Biomarker for Oral Squamous Cell Carcinoma. *Frontiers in Bioengineering and Biotechnology*. 2022;9.
14. Li Q, Dong C, Cui J, Wang Y, Hong X. Over-expressed lncRNA HOTAIRM1 promotes tumor growth and invasion through up-regulating HOXA1 and sequestering G9a/EZH2/Dnmts away from the HOXA1 gene in glioblastoma multiforme. *J Exp Clin Cancer Res*. 2018;37(1):265.
15. Ye L, Meng X, Xiang R, Li W, Wang J. Investigating function of long noncoding RNA of HOTAIRM1 in progression of SKOV3 ovarian cancer cells. *Drug Dev Res*. 2021;82(8):1162-1168.
16. Kim HK, Bhattarai KR, Junjappa RP, et al. TMBIM6/BI-1 contributes to cancer progression through assembly with mTORC2 and AKT activation. *Nat Commun*. 2020;11(1):4012.
17. Wu F, Gao P, Wu W, et al. STK25-induced inhibition of aerobic glycolysis via GOLPH3-mTOR pathway suppresses cell proliferation in colorectal cancer. *J Exp Clin Cancer Res*. 2018;37(1):144.
18. Yang X, Hei C, Liu P, et al. Inhibition of mTOR pathway by rapamycin reduces brain damage in rats subjected to transient forebrain ischemia. *Int J Biol Sci*. 2015;11(12):1424-1435.
19. Blagden S, Omlin A, Josephs D, et al. First-in-human study of CH5132799, an oral class I PI3K inhibitor, studying toxicity, pharmacokinetics, and pharmacodynamics, in patients with metastatic cancer. *Clin Cancer Res*. 2014;20(23):5908-5917.
20. Weng ML, Chen WK, Chen XY, et al. Fasting inhibits aerobic glycolysis and proliferation in colorectal cancer via the Fdft1-mediated AKT/mTOR/HIF1alpha pathway suppression. *Nat Commun*. 2020;11(1):1869.
21. Li J, Cheng D, Zhu M, et al. OTUB2 stabilizes U2AF2 to promote the Warburg effect and tumorigenesis via the AKT/mTOR signaling pathway in non-small cell lung cancer. *Theranostics*. 2019;9(1):179-195.
22. Zheng YL, Li L, Jia YX, et al. LINC01554-mediated glucose metabolism reprogramming suppresses Tumorigenicity in hepatocellular carcinoma via downregulating PKM2 expression and inhibiting Akt/mTOR signaling pathway. *Theranostics*. 2019;9(3):796-810.
23. McKinley ET, Bugaj JE, Zhao P, et al. 18FDG-PET predicts pharmacodynamic response to OSI-906, a dual IGF-1R/IR inhibitor, in preclinical mouse models of lung cancer. *Clin Cancer Res*. 2011;17(10):3332-3340.
24. Shen Y, Xu J, Pan X, et al. LncRNA KCNQ1OT1 sponges miR-34c-5p to promote osteosarcoma growth via ALDOA enhanced aerobic glycolysis. *Cell Death Dis*. 2020;11(4):278.

25. Shen Y, Zhao S, Wang S, et al. S1P/S1PR3 axis promotes aerobic glycolysis by YAP/c-MYC/PGAM1 axis in osteosarcoma. *EBioMedicine*. 2019;40:210-223.
26. Pan X, Tan J, Tao T, et al. LINC01123 enhances osteosarcoma cell growth by activating the hedgehog pathway via the miR-516b-5p/Gli1 axis. *Cancer Sci*. 2021;112(6):2260-2271.
27. Zhao SJ, Shen YF, Li Q, et al. SLIT2/ROBO1 axis contributes to the Warburg effect in osteosarcoma through activation of SRC/ERK/c-MYC/PFKFB2 pathway. *Cell Death Dis*. 2018;9(3):390.
28. Shen W, Song Z, Zhong X, et al. Sangerbox: a comprehensive, interaction-friendly clinical bioinformatics analysis platform. *iMeta*. 2022;1(3):e36.
29. Tong WH, Sourbier C, Kovtunovych G, et al. The glycolytic shift in fumarate-hydratase-deficient kidney cancer lowers AMPK levels, increases anabolic propensities and lowers cellular iron levels. *Cancer Cell*. 2011;20(3):315-327.
30. Shen S, Yao T, Xu Y, Zhang D, Fan S, Ma J. CircECE1 activates energy metabolism in osteosarcoma by stabilizing c-Myc. *Mol Cancer*. 2020;19(1):151.
31. Shin N, Lee HJ, Sim DY, et al. Apoptotic effect of compound K in hepatocellular carcinoma cells via inhibition of glycolysis and Akt/mTOR/c-Myc signaling. *Phytother Res*. 2021;35(7):3812-3820.
32. Masui K, Tanaka K, Akhavan D, et al. mTOR complex 2 controls glycolytic metabolism in glioblastoma through FoxO acetylation and upregulation of c-Myc. *Cell Metab*. 2013;18(5):726-739.
33. Hu LP, Zhang XX, Jiang SH, et al. Targeting purinergic receptor P2Y2 prevents the growth of pancreatic ductal adenocarcinoma by inhibiting cancer cell glycolysis. *Clin Cancer Res*. 2019;25(4):1318-1330.
34. Jin J, Kim C, Xia Q, et al. Activation of mTORC1 at late endosomes misdirects T cell fate decision in older individuals. *Sci Immunol*. 2021;6(60):eabg0791.
35. Ding L, Liu T, Qu Y, et al. lncRNA MELTF-AS1 facilitates osteosarcoma metastasis by modulating MMP14 expression. *Mol Ther Nucleic Acids*. 2021;26:787-797.
36. Shi D, Wu F, Mu S, et al. LncRNA AFAP1-AS1 promotes tumorigenesis and epithelial-mesenchymal transition of osteosarcoma through RhoC/ROCK1/p38MAPK/Twist1 signaling pathway. *J Exp Clin Cancer Res*. 2019;38(1):375.
37. Salmena L, Poliseno L, Tay Y, Kats L, Pandolfi PP. A ceRNA hypothesis: the Rosetta stone of a hidden RNA language? *Cell*. 2011;146(3):353-358.
38. Lin YH, Guo L, Yan F, Dou ZQ, Yu Q, Chen G. Long non-coding RNA HOTAIRM1 promotes proliferation and inhibits apoptosis of glioma cells by regulating the miR-873-5p/ZEB2 axis. *Chin Med J (Engl)*. 2020;133(2):174-182.
39. Ahmadov U, Picard D, Bartl J, et al. The long non-coding RNA HOTAIRM1 promotes tumor aggressiveness and radiotherapy resistance in glioblastoma. *Cell Death Dis*. 2021;12(10):885.
40. Zheng M, Wang YH, Wu XN, et al. Inactivation of Rheb by PRAK-mediated phosphorylation is essential for energy-depletion-induced suppression of mTORC1. *Nat Cell Biol*. 2011;13(3):263-272.
41. Zhang Y, Gao X, Saucedo LJ, Ru B, Edgar BA, Pan D. Rheb is a direct target of the tuberous sclerosis tumour suppressor proteins. *Nat Cell Biol*. 2003;5(6):578-581.
42. Velica P, Zech M, Henson S, et al. Genetic regulation of fate decisions in therapeutic T cells to enhance tumor protection and memory formation. *Cancer Res*. 2015;75(13):2641-2652.
43. Wan G, Xie W, Liu Z, et al. Hypoxia-induced MIR155 is a potent autophagy inducer by targeting multiple players in the MTOR pathway. *Autophagy*. 2014;10(1):70-79.
44. Bommareddy A, Hahm ER, Xiao D, et al. Atg5 regulates phenethyl isothiocyanate-induced autophagic and apoptotic cell death in human prostate cancer cells. *Cancer Res*. 2009;69(8):3704-3712.
45. Chen Y, Lu Y, Ren Y, et al. Starvation-induced suppression of DAZAP1 by miR-10b integrates splicing control into TSC2-regulated oncogenic autophagy in esophageal squamous cell carcinoma. *Theranostics*. 2020;10(11):4983-4996.
46. Dong P, Wang X, Liu L, et al. Dampened VEPH1 activates mTORC1 signaling by weakening the TSC1/TSC2 association in hepatocellular carcinoma. *J Hepatol*. 2020;73(6):1446-1459.
47. Yu J, Henske EP. Estrogen-induced activation of mammalian target of rapamycin is mediated via tuberin and the small GTPase Ras homologue enriched in brain. *Cancer Res*. 2006;66(19):9461-9466.
48. Han T, Zhan W, Gan M, et al. Phosphorylation of glutaminase by PKCepsilon is essential for its enzymatic activity and critically contributes to tumorigenesis. *Cell Res*. 2018;28(6):655-669.
49. Jiang SH, Li J, Dong FY, et al. Increased serotonin signaling contributes to the Warburg effect in pancreatic tumor cells under metabolic stress and promotes growth of pancreatic tumors in mice. *Gastroenterology*. 2017;153(1):277-291 e19.
50. Mi YJ, Geng GJ, Zou ZZ, et al. Dihydroartemisinin inhibits glucose uptake and cooperates with glycolysis inhibitor to induce apoptosis in non-small cell lung carcinoma cells. *PLoS One*. 2015;10(3):e0120426.
51. Peng W, Huang W, Ge X, Xue L, Zhao W, Xue J. Type Igamma phosphatidylinositol phosphate kinase promotes tumor growth by facilitating Warburg effect in colorectal cancer. *EBioMedicine*. 2019;44:375-386.
52. Li Z, Ge Y, Dong J, et al. BZW1 facilitates glycolysis and promotes tumor growth in pancreatic ductal adenocarcinoma through potentiating eIF2alpha phosphorylation. *Gastroenterology*. 2022;162(4):1256-1271 e14.

SUPPORTING INFORMATION

Additional supporting information can be found online in the Supporting Information section at the end of this article.

How to cite this article: Yu X, Duan W, Wu F, et al. LncRNA-HOTAIRM1 promotes aerobic glycolysis and proliferation in osteosarcoma via the miR-664b-3p/Rheb/mTOR pathway. *Cancer Sci*. 2023;114:3537-3552. doi:10.1111/cas.15881